Collective Dynamics of Terminally Anchored Polymer Chains

Spiros H. Anastasiadis†*

Foundation for Research and Technology-Hellas, Institute of Electronic Structure and Laser, P.O. Box 1527, 71110 Heraklion, Crete, Greece

Abstract: Thermal fluctuations of the segment density profile of a polymer brush were probed by dynamic light scattering in the evanescent wave configuration; the time correlation functions of concentration fluctuations with wavevector q were measured. It is found that there is a preferred wavelength of the order of the brush thickness, L_0, of these fluctuations with a concurrent slowing down of their thermal decay rate. A theory is presented for the small-amplitude deformation of the free surface of a parabolic brush in solution; a maximum in the respective structure factor of the concentration fluctuations is predicted at $q^* L_0 \sim O(1)$, in agreement with the experiment.

INTRODUCTION

Polymer adsorption has numerous consequences in disciplines from biology to tribology and technological applications like surface/interface modification, adhesion and wetting, and stabilization of colloids. Selective adsorption from solution via attaching the ends of polymer chains onto a solid surface can lead to a grafted layer due to chain extension away from the surface, a configuration termed a polymer brush (Ref. 1); this configuration of stretched tethered chains is a model structure for a large variety of confined polymer systems (Ref. 2). Most of the theoretical and experimental work, so far, have addressed the static structure of tethered chains (Refs. 2-7), whereas the absence of direct experimental observation of their dynamic structure together with the strong relevant theoretical predictions available (Refs. 3,8) invite new experimental efforts in this active field (Ref. 5).

In this work, the time correlation functions of composition fluctuations at thermal equilibrium are measured in poly(ethylene oxide)-*block*-polystyrene block copolymers, PEO-PS, adsorbed from toluene solution onto a glass surface with their short PEO blocks (Ref. 9). The evanescent electromagnetic wave, produced under total reflection of a laser beam, is utilized as the incident beam in the scattering experiment; the time correlation functions $C(q,t)$ of concentration fluctuations with wavevector q are obtained taking advantage of the broad time range (10^{-7}-10^{3} s) of photon correlation spectroscopy (PCS) (Ref. 10). Besides the applicability of the evanescent wave dynamic light scattering (EWDLS) to dynamics study of tethered chains (Ref. 9), the experiments demonstrate that long-lived fluctuations possess a finite wavelength of $O(L_0)$ as indicated by the apparent maximum in the scattering intensity at a finite wavevector, q^*. These observations indicate that the fluctuations observed may be associated with a small-amplitude deformation of the free surface of the brush (Ref. 11). We

† In collaboration with G. Fytas, D. Vlassopoulos, A. Likhtman, A. N. Semenov, C. Toprakcioglu, J. Li, B. Factor, R. Seghrouchni, W. Theobald.

* Also at University of Crete, Physics Department, 711 03 Heraklion Crete, Greece.

 CCC 1022-1360/99/$ 17.50+.50/0

present a theory (Ref. 12) for the calculation of the excess Helmholtz energy of a small sinusoidal deformation of the free surface of a parabolic brush in solution and show that there is a maximum in the respective structure factor of the concentration fluctuations at $q^* L_0 \sim O(1)$; this is due to a balance between elastic and concentration gradient contributions to the Helmholtz energy functional.

EXPERIMENTAL

The detailed material and surface characterization is essential for the interpretation of the results obtained from this new experimental technique. The PEO-PS model system in toluene was selected due to the extensive information on the adsorbed amount, kinetics of adsorption, and segment density profiles obtained from ellipsometry, neutron reflectivity, and surface balance experiments (Ref. 7). The characteristics of the PEO-PS diblocks and the brush-like grafted layers are given in Table 1. The brush is formed by the stretched PS block dangling in the solution; the anchoring density is $\sigma = s^{-2}$ (chains nm^{-2}), with s denoting the interanchor spacing. The equilibrium thickness L_0 of the grafted PS monolayer corresponds to a parabolic density profile normal to the surface (Refs. 1a, 7c). The adsorption conditions of Ref. 7 were reproduced, and the copolymer concentration for maximum adsorption A^* was used; equilibrium was confirmed by the stability of the scattered intensity. The temperature throughout the experiments was 23 °C.

Table 1. Molecular and brush characteristics of the PEO-PS in toluene (Ref. 7)

Code	M_W	N_{PS}	N_{PEO}	A^* mg m^{-2}	L_0 nm	s nm
PEO-PS/80	80 000	730	90	2.9	45±3	7±0.5
PEO-PS/150	150 000	1420	51	1.6	70±5	2±0.5
PEO-PS/184	184 000	1700	167	2.6	80±5	11±0.5
PEO-PS/500	502 000	4790	91	1.7	130±10	23±1

The experimental set-up is schematically presented in Fig. 1. Note that few attempts to measure dynamic properties of strong scatterers (e.g., colloidal particles) close to a wall by EWDLS have been reported (Ref. 13). For weak scattering, however, careful optical alignment to minimize parasitic scattering and specific control experiments to ensure homodyne detection for both static and dynamic measurements are crucial for the quality of the experimental functions (Ref. 10) and in order to verify that the standard assertions used in bulk solution measurements by PCS are accurate for the present EWDLS.

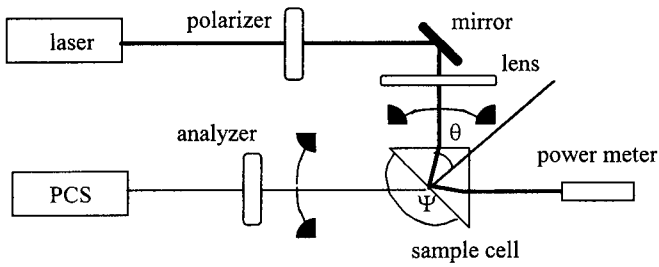

Fig. 1. Schematic of the evanescent wavedynamic light scattering instrumentation (Ref. 9). The light scattering cell is a right-angled high-refractive-index prism to which a semicylindrical cell is epoxy-glued.

The evanescent wave geometry is shown in Fig. 2. For total reflection $[\theta > \theta_c = \arcsin(n_2 / n_1)]$, the evanescent wave propagating parallel to the surface, with an electric field exponentially decaying away from the surface and with penetration depth ζ, is scattered by the concentration fluctuations of wavevector $\mathbf{q}$ ($|\mathbf{q}| = 2k_i \sin(\Psi/2)$) in the adsorbed polymer layer.

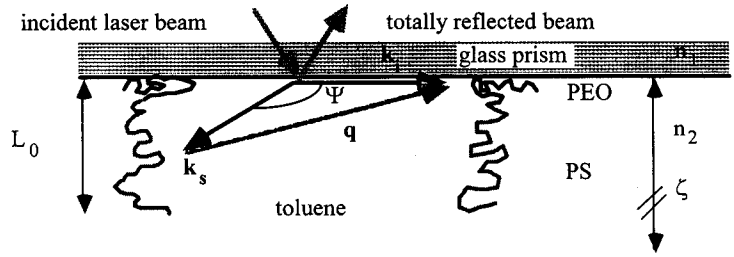

Fig. 2. The evanescent wave geometry versus the polymer brush (Ref. 9).

The measured intensity autocorrelation function $G(q,t)$ leads to the computation of the desired $|C(q,t)|^2 = (G(q,t) - A)/f$, where A is the baseline at sufficiently long delay times and f is a coherence (instrumental) factor.

RESULTS AND DISCUSSION

Figure 3 shows $C(q,t)$ for the tethered PS layers. The featureless $C(q,t)$ from pure toluene, as expected, becomes a well defined decay function after a 7-h counting time for PEO-PS/500 at q = 0.034 nm^{-1}. This surface relaxation function clearly reflects the dynamics of the grafted layer and not fluctuations due to the translational motion of free polymer chains (solid line) measured in the "bulk"geometry obtained in situ for $\theta = \theta_C + 5^\circ$, where the incident light penetrates into the solution as a refracted beam. $C(q,t)$ is well represented by a single exponential function

$$C(q,t) = a(q)\exp[-\Gamma(q)t] \tag{1}$$

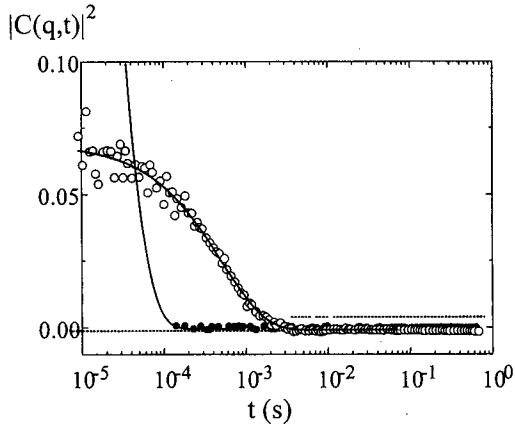

Fig. 3. $C(q,t)$ for toluene (●) and for the PEO-PS/500 brush in toluene (0.4 mg/ml and 23 °C) at q=0.034 nm^{-1} (O), and the distinctly different correlation function from the "bulk" PEO-PS/500 solution (—).

where $\Gamma(q)$ is the thermal decay rate of the composition fluctuations in the layer. The value of the relaxation amplitude $a(q)$ shows that about 25 % of the total scattering intensity, I_{tot}, is due to the probed polymer layer mode. Both $C(q,t)$ and the process intensity $I(q) = a(q)I_{tot}$ depend on the scattering wavevector q (Ref. 9), where $I(q)$ increases with q (Fig. 4), implying strong suppression of the low wavevector (long wavelength) fluctuations, whereas $\Gamma(q)$ for all but the longest PEO-PS chain is virtually insensitive to q; for PEO-PS/500, a slowing down of the rate is observed at high wavevectors. The intensity data for the four different layers superimpose well when $I(q)$ is divided by A^* and q is normalized to L_0 (Fig. 4). Actually, the reduced intensities $I(q) / A^*$ for all layers are found to exhibit a $(qL_0)^2$ dependence in the lower experimental qL_0 range (~1-4; Fig. 4); for the longest PEO-PS/500 layer and at higher qL_0 values, $I(q)$ exhibits a higher rate of increase with q with indications of a broad maximum at the edge of the highest accessible q range.

Theory predicts the end-to-end chain relaxation for a grafted brush to depend on N and on the anchoring density σ (Ref. 8). Considering mean-squared fluctuations of the chain free end in the perpendicular direction proportional to L_0^2, a Rouse-like diffusion led to the characteristic q-independent relaxation rate

$$\Gamma \propto w(\sigma)\sigma^{-\beta}N^{-3} \tag{2}$$

with $w(\sigma)$ denoting the microscopic mobility (can depend on σ), and β = 2/3 for free-draining chains or β = 1 when hydrodynamic interactions are taken into account (Ref. 8b). Molecular dynamics and Monte-Carlo simulations (Ref. 14) were consistent with the scaling prediction of Eq. 2.

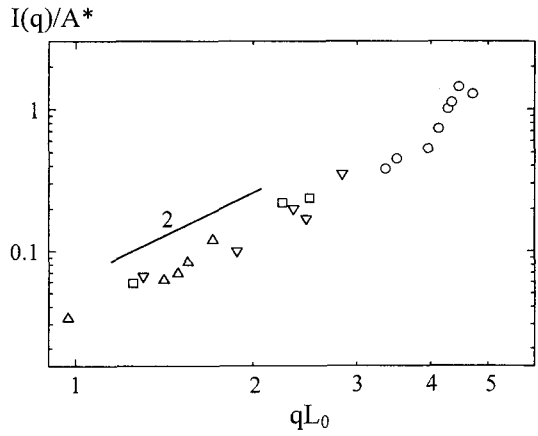

Fig. 4. Variation of the intensity normalized to the adsorbed mass per area, A^*, for all four brushes with the product of the wavevector times the layer thickness: Δ PEO-PS/80, □ PEO-PS/150, ∇ PEO-PS/184, O PEO-PS/500. (The line has slope 2.)

Dynamic light scattering probes collective dynamics. Thus, the experimental $\Gamma(q)$ shows the effect of thermodynamics, i.e., of $I(q)$. Therefore, $\Gamma(q)$ is q-independent for the three shorter brushes and shows a slowing down for PEO-PS/500 at high wavevectors. The N-

dependence of $\Gamma(q)$ at low qL_0 (Eq. 2) is revealed when the dependence of the microscopic mobility on concentration (and thus on σ) is taken into account.

Recently, small-amplitude deformation of the free surface of an incompressible, molten „step function" polymer brush was analyzed and the Helmholtz energy, F, relative to that of the undeformed flat layer was computed (Ref. 11). Both lateral and perpendicular chain displacements were considered and the correlation function $P(q)$ of height fluctuations at the surface exhibited a maximum at a certain value of $q^* L_0$ since both long- and short-wavelength fluctuations are suppressed at the entropic and interfacial tension (γ) expense, respectively. This led to a preferred wavelength (parallel to the polymer/air interface) $2\pi / q^*$ of the most probable thermally-excited surface modes. The value of $q^* L_0$ depends on the relative contributions to F of the γ-term at high q versus that due to chain stretching. Relaxing the assumption that all free chain ends reside at the top layer surface (Ref. 11b) leads to only a slight modification.

We have extended (Ref. 12) the earlier work for the case of small-amplitude deformation of the free surface of a parabolic brush in solution (Fig. 5) by calculating the contributions to the Helmholtz energy of the elastic term due to chain stretching and of a gradient contribution to the non-constant concentration in both x and z directions, where straight chain trajectories were assumed.

In each wedge (Fig. 5), the molecular field is a parabolic function of the distance from the junction point along the chain, $h(x)$, i.e., $U = A - B[l(x)]^2$, where $l^2(x) = z^2(1+f^2(x))$, $f(x)$ is the tangent of the angle between the chain trajectory and the perpendicular to the plane z = 0 (z is the axis perpendicular to the grafting plane), $h(x)$ is the height of the brush, $\{x + f(x)h(x), h(x)\}$ are the coordinates of the free chain end, and $\phi(x,z) = -U/\omega$ is the density of polymer chains, ω being the excluded volume parameter. The polymer density should be zero at the brush edge, $z = h(x)$, i.e., $\phi(h(x)) = A(x) - Bh^2(x)\left(1 + f^2(x)\right) = 0$, whereas the total amount of polymer inside one wedge must be equal to the number of grafted monomer units, $N\sigma$: $\int_{\text{wedge}} \phi(x,z)\mathrm{d}z = N\sigma$.

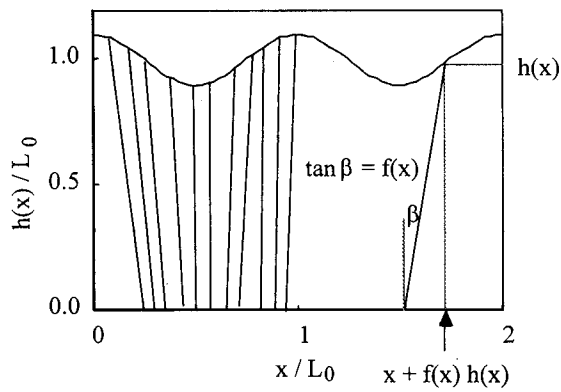

Fig. 5. Schematic diagram of the geometry of a deformed polymer brush in solution.

Since there are three unknown functions and only two equations, one needs to predefine one of the unknowns; it is assumed that the function $f(x) = -(8\varepsilon/(qL_o))\sin(qx)$. Then, one gets $h(x) = L_o\left(1 + \varepsilon\cos(qx) + O(\varepsilon^2)\right)$ with $L_o = (24/\pi^2)^{1/3} N(\sigma\omega\alpha^2)^{1/3}$, and $\alpha = b/\sqrt{6}$ where b is the statistical segment length. The total elastic Helmholtz energy per unit area is then

$$\frac{F_{\text{elastic}}}{F_0} = 1 + \varepsilon^2\left(\frac{7}{2} + \frac{160}{9q^2h_0^2}\right) \tag{3}$$

with $F_o = (9/10)\left(\pi^2/24\right)^{1/3} N\sigma(\sigma\omega/\alpha)^{2/3}$ is the Helmholtz energy of the undeformed brush. The gradient term contribution to the Helmholtz energy per surface area is calculated as

$$F_{\text{gradient}} = \frac{\alpha^2}{4}\frac{q}{2\pi}\int_0^h dz \int_0^{2\pi/q} dx \frac{(\nabla\phi)^2}{\phi} =$$

$$= \frac{\pi^2 L_0}{16N^2\omega}\left\{\left(1 + \frac{1}{2}\ln\frac{2}{\delta}\right)\left[1 + \frac{64\varepsilon^2}{3(qL_0)^2} + \frac{3\varepsilon^2}{2}\right] + \varepsilon^2\frac{(qL_0)^2}{4}\ln\frac{2}{\delta} - 2\varepsilon^2\left[-\ln(2\delta) - 1\right]\right\} \tag{4}$$

where $\delta = \xi/h_0 = N^{2/3}(a/h_0)^{4/3} = N^{-2/3}[a/(\sigma\omega)]^{4/9} << 1$ with $\xi \cong \alpha^{4/3}N^{2/3}/L_o^{-1/3}$ being the terminal correlation length (Ref. 16).

The final result can be presented in the form $F = F_0 + \frac{1}{2}(\Delta\Phi)^2[S(q)]^{-1}$ with $\Phi = \int_0^h \phi(x,z)dz$ and $\Delta\Phi \equiv \Phi - \Phi_0 = 3N\sigma\varepsilon$, where the structure factor of the fluctuations of total concentration in the brush is

$$[S(q)]^{-1} = \frac{1}{5}\left(\frac{\pi^2}{24}\right)^{1/3}\left(\frac{\omega\sigma}{\alpha}\right)^{2/3}\frac{1}{N\sigma}\left\{\frac{7}{2} + \frac{160}{9(qL_o)^2} + \frac{5(3\pi)^{2/3}\ln(2/\delta)}{72}\left(\frac{\alpha}{\omega\sigma}\right)^{4/3}\frac{(qh_0)^2}{N^2}\right\} \tag{6}$$

Thus, theory predicts a preferable q^* for maximum fluctuations at

$$q^*L_0 = \left[\frac{256}{(3\pi)^{2/3}\ln(2/\delta)}\right]^{1/4} N^{1/2}\left(\frac{\sigma\omega}{a}\right)^{1/3} \tag{7a}$$

i.e., at

$$q^* = \frac{2}{3^{1/2}[\ln(2/\delta)]^{1/4}}\frac{1}{\alpha N^{1/2}} \tag{7b}$$

Actually, the predicted value for q^* for the PEO-PS/500 copolymer is $q^* \cong 0.039$ nm^{-1}, right near the edge of our experimental q range. At low wavevectors,

$$S(qL_o \to 0) = 0.38\left(\frac{\omega\sigma}{\alpha}\right)^{-2/3} N\sigma(qL_o)^2 \tag{8}$$

in agreement with the behavior of the experimental data (Fig. 4). Note that $A^* = N\sigma$. Currently, the theory is being extended for the calculation of the full dynamic structure factor $S(q,t)$, i.e., including its temporal dependence.

Summarizing, the evanescent wave dynamic light scattering technique allowed the investigation of the dynamic structure of terminally anchored PS layers, which revealed the presence of long-lived thermally induced layer fluctuations with wavelength $2\pi/q^* \cong 1.3L_0$ indicating strong surface coverage effects on their thermal decay rate. The identification of

the precise mechanism of the layer fluctuations would highly benefit from a theoretical calculation of the full structure factor $S(q,t)$. This will promote fundamental studies of polymers near surfaces and provide information on chain relaxation and brush friction, relevant to technological applications.

ACKNOWLEDGEMENTS

Part of this research was sponsored by the European Union (International Scientific Cooperation, Contract ISC*CT93-0951) and by NATO's Scientific Affairs Division (Science for Stability Programme).

REFERENCES

1. (a) S. T. Milner, *Science* **251**, 905 (1991); (b) R. Yerushalmi-Rozen and J. Klein, *Phys. World* 1995 (August), 30.
2. A. Halperin, M. Tirrell, T.P. Lodge, *Adv. Polym. Sci.* **100**, 31, (1992).
3. (a) P. G. de Gennes, *Adv. Colloid Interface Sci.* **27**, 189 (1987); (b) P. G. de Gennes, *C.R. Acad. Sci., Ser. II* **302**, 765 (1986).
4. H. E. Johnson and S. Granick, *Science* **255**, 966 (1992).
5. J. T. Koberstein (Ed.), *Polymer Surfaces and Interfaces*, *MRS Bull.* **21**, 16 (1996).
6. B. Farago, M. Monkenbusch, D. Richter, J. S. Huang, L. J. Fetters, A. P. Gast, *Phys. Rev. Lett.* **71**, 1015 (1993).
7. (a) H. J. Taunton, C. Toprakcioglu, L. J. Fetters, J. Klein, *Macromolecules* **23**, 571, (1990); (b) H. Motschmann, M. Stamm, C. Toprakcioglu, *Macromolecules* **24**, 3691 (1991); (c) J. B. Field, C. Toprakcioglu, R. C. Ball, H. B. Stanley, L. Dai, W. Barford, *Macromolecules* **25**, 434, (1992).
8. (a) A. Halperin and S. Alexander, *Europhys. Lett.* **6**, 329 (1988); (b) L. I. Klushin and A. M. Skvortsov, *Macromolecules* **24**, 1549 (1991).
9. G. Fytas, S. H. Anastasiadis, R. Seghrouchni, D. Vlassopoulos, J. Li, B. J. Factor, W. Theobald, and C. Toprakcioglu, *Science* **274**, 2041 (1996)
10. G. Fytas and G. Meier in *Dynamic Light Scattering. The Method and Some Applications* (W. Brown, Ed.), Oxford Clarendon Press, London, 1993.
11. (a) G. H. Fredrickson, A. Ajdari, L. Leibler, J. P. Carton, *Macromolecules* **25**, 2882 (1992); (b) H. W. Xi and S. T. Milner, *Macromolecules* **29**, 4772 (1996); (c) F. J. Solis and G. T. Pickett, *Macromolecules* **28**, 4307 (1995); (d) D. Long, A. Ajdari, L. Leibler, *Langmuir* **12**, 1675 (1996).
12. A. E. Likhtman, S. H. Anastasiadis, and A. N. Semenov, *Macromol. Theory Simul.*, submitted .
13. K. H. Lan, N. Ostrowsky, D. Sornette, *Phys. Rev. Lett.* **57**, 17 (1986).
14. (a) M. Murat and G. S. Grest, *Macromolecules* **22**, 4054 (1989); (b) P. Y. Lai and K. Binder, *J. Chem. Phys.* **95**, 9288 (1991).
15. S. Milner, *Macromolecules* **21**, 2610 (1988).
16. A. N. Semenov, *Macromolecules* **25**, 2273 (1992).